AIIM

Association for Information and Image Management

1100 Wayne Avenue, Suite 1100
Silver Spring, Maryland 20910

301/587-8202

Centimeter

Inches

1 of 1

Conf-9409202--1

SAND94-1999C

Quartz Resonator Fluid Monitors for Vehicle Applications*

*R. W. Cernosek, S. J. Martin, K. O. Wessendorf, M. D. Terry and A. N. Rumpf***

Sandia National Laboratories
P. O. Box 5800, M/S 0351
Albuquerque, NM 87185-0351
(505) 845-8818

Abstract

Thickness shear mode (TSM) quartz resonators operating in a new "Lever oscillator" circuit are used as monitors for critical automotive fluids. These monitors respond to the density and viscosity of liquids contacting the quartz surface. Sensors have been developed for determining the viscosity characteristics of engine lubricating oil, the state-of-charge of lead-acid storage batteries, and the concentration variations in engine coolant.

Introduction

Fluids play an extremely important role in today's automotive systems. They serve as fuels, lubricants, coolants, cleaners, hydraulic agents, and charge media. When a fluid depletes, whether it is through consumption or loss, through degradation to the point of nonfunctionality, or through contamination with foreign matter, critical vehicle systems can cease operation or, worse yet, suffer catastrophic damage. It is imperative that automotive fluids be maintained. However, few vehicles have diagnostic sensors, aside from fuel and oil pressure gauges, to assist the driver/operator in assessing fluid capacity. One must still visually inspect fluid levels using dipsticks and filler marks and provide fluid replacement at intervals dictated by the odometer or calendar.

In this paper we describe a quartz resonator technology that has the capability to sense physical parameters of a contacting medium. The monitor responds to the density and viscosity of a liquid, measures accumulated surface mass, senses phase changes in the contacting material, and can determine viscoelastic properties of the medium. It can also simply respond to the presence or absence of a fluid. Sensors can be configured for *in situ* use in most environments, and the device response is provided in real-time. These characteristics make the quartz resonator monitor useful not only as a vehicle sensor but also as a diagnostic tool for component or system evaluations and qualifications in the laboratory.

Quartz resonators have been partially characterized in three automotive fluid environments: engine lubricating oil, lead-acid battery electrolyte, and engine coolant (ethylene glycol). Details of these evaluations are provided in the following sections. The diagnostic ability for the sensor in these fluids is preliminary yet promising. Because of the large viscosities encountered in some of the target liquids, a new oscillator electronic circuit was designed to operate with the quartz resonators. Brief descriptions of this circuit are also provided in the paper.

Quartz Resonator Sensors

The typical thickness shear mode (TSM) quartz resonator is shown in Fig. 1. Metal electrodes (few hundred nanometers thick) are deposited on each face of a thin wafer of AT-cut quartz. Applying an RF voltage to the electrodes induces a strain in the piezoelectric quartz. Because of the orientation of the crystal axes and the direction of the applied field,

* This work was performed at Sandia National Laboratories supported by the U. S. Department of Energy under contract No. DE-AS04-94AL85000.

** On Contract from Ktech Corporation, Albuquerque, NM.

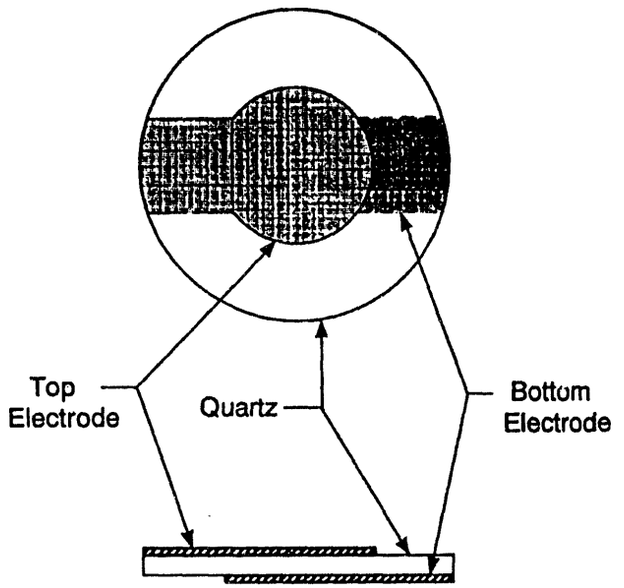

Fig. 1. Top and edge views of a TSM quartz resonator.

shear displacement occurs (see Fig. 2). The amplitude of the planar displacement in the x-direction, u_x, as a function of time, t, and position along the quartz thickness, y, is given by [1]

$$u_x(y,t) = \left(A e^{j\beta_q y} + B e^{j\beta_q y}\right) e^{j\omega t} \qquad (1)$$

where A and B are constants, $\omega = 2\pi f$ is the angular excitation frequency, β_q is the wavenumber describing the shear wave propagation in the quartz, and $j = (-1)^{1/2}$. Solving Eq. (1) subject to the boundary conditions at the upper and lower surfaces gives sinusoidal standing waves of odd mode number: $\beta_q = N\pi/h$, N = 1, 3, 5, ..., where h the quartz thickness. In the unperturbed state (no surface loading), the resonant frequency, f_s, is

$$f_s = \frac{N v}{2h} = \frac{N}{2h}\sqrt{\frac{\mu_q}{\rho_q}} \qquad (2)$$

where v is the shear wave propagation (phase) velocity in the quartz, μ_q is the quartz shear stiffness, and ρ_q is the quartz density.

Any material in contact with one or both surfaces of the quartz will perturb the resonator. The acoustic wave extends into the contacting material. An ideal mass layer, as shown in Fig. 2, acts as a rigid medium and moves synchronously with the oscillating quartz surface. The resonant frequency of the device is reduced from f_s due to added material thickness and a change in density. No loss of resonant magnitude is experienced due to an ideal mass layer.

Liquid in contact with the resonator surface is viscously-entrained. The liquid velocity field, $v_x(y,t)$, is determined from the one-dimensional Navier-Stokes equation [2]:

$$\eta\frac{\partial^2 v_x}{\partial y^2} = \rho\frac{\partial v_x}{\partial t} \qquad (3)$$

where ρ and η are the fluid density and viscosity. The solution to Eq. (3) for a shear driving force at the solid-liquid interface is [2]

$$v_x(y,t) = v_{xo}\, e^{-\gamma y}\, e^{j\omega t} \qquad (4)$$

where v_{xo} is the particle velocity at the quartz surface and γ is the propagation constant for the damped shear wave radiated into the fluid. For a Newtonian fluid (viscosity independent of shear rate), the propagation constant, found by substituting Eq. (4) into Eq. (3), is given by

$$\gamma = \frac{1+j}{\delta} \qquad (5)$$

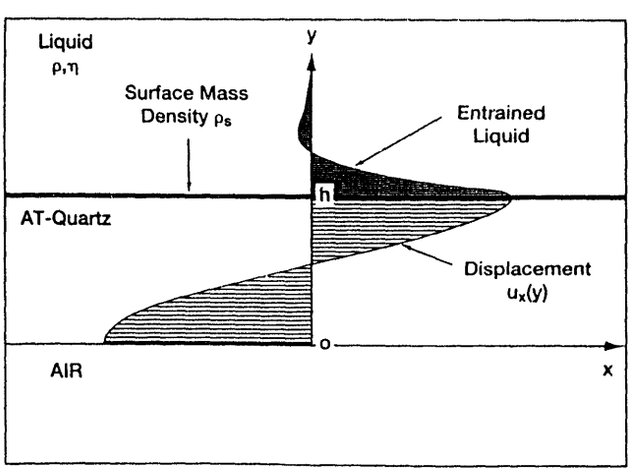

Fig. 2. Cross-sectional view of a smooth TSM resonator with the upper surface contacted by an ideal mass layer and a viscously-entrained Newtonian liquid.

with the decay length, δ, defined by [3]

$$\delta \equiv \sqrt{\frac{2\eta_l}{\omega\rho}} \qquad (6)$$

The complex propagation constant creates both oscillatory and dissipative factors in the velocity field of Eq. (4), giving rise to a frequency shift and magnitude damping of the acoustic wave.

An equivalent-circuit model (Fig. 3) can be used to describe the electrical response of both the unperturbed and loaded TSM resonator [4]. The model consists of a "static" branch containing C_o, the capacitance created by the electrodes across the insulating quartz, and C_p, the parasitic capacitance of the mounting fixture, in parallel with a "motional" branch produced by the mechanically-vibrating quartz. For the unperturbed resonator, the motional impedance, Z_m, is given by

$$Z_m\,(\text{unperturbed}) = R_1 + j\omega L_1 + \frac{1}{j\omega C_1} \qquad (7)$$

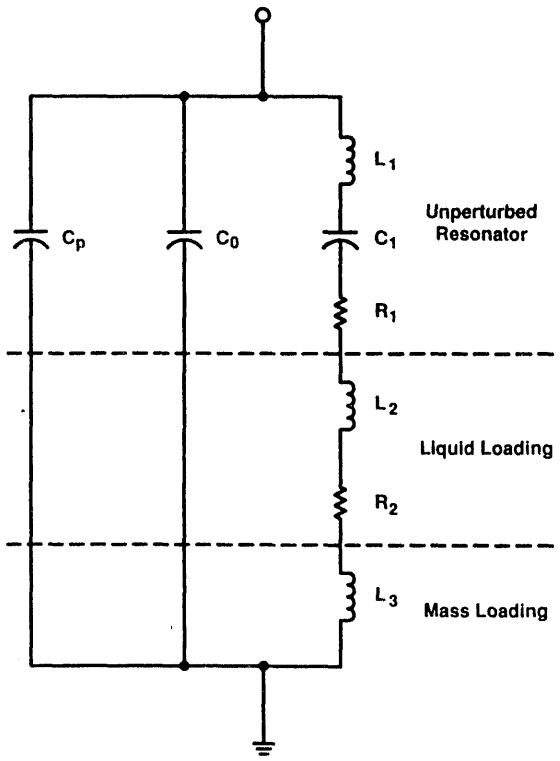

Fig. 3. Equivalent-circuit model describing the electrical characteristics of a TSM resonator having both mass and liquid loading.

with [4]

$$C_1 = \frac{8K^2 C_o}{(N\pi)^2} \qquad (8)$$

$$R_1 = \frac{\eta_q}{\mu_q C_1}\left(\frac{\omega}{\omega_s}\right)^2 \qquad (9)$$

and

$$L_1 = \frac{1}{\omega_s^2 C_1} \qquad (10)$$

where η_q is the quartz viscosity, $\omega_s = 2\pi f_s$ is angular series resonant frequency, and K^2 is the quartz electromechanical coupling factor. The series resonant frequency is defined by

$$f_s \equiv \frac{\omega_s}{2\pi} = \frac{1}{2\pi\sqrt{L_1 C_1}} \qquad (11)$$

The minimum resonant impedance is limited by the motional resistance, R_1, and the capacitive reactance in the static branch. Quality factors, Q, for unperturbed quartz resonators often exceed 10^5.

An ideal surface mass layer contributes only to energy storage in the resonator system. The motional impedance for this term is [4]

$$Z_m\,(\text{mass}) = j\omega L_3 = j\omega \frac{2n\omega_s L_1 \rho_s}{N\pi\sqrt{\mu_q \rho_q}} \qquad (12)$$

where n is the number of sides (1 or 2) containing the mass layer and ρ_s is the surface mass density (mass/area).

Liquid loading adds both an energy storage and a power dissipation element to the motional branch. The motional impedance due to the liquid is given by

$$Z_m\,(\text{liquid}) = R_2 + j\omega L_2 \qquad (13)$$

with [4]

$$R_2 = \frac{n\omega_s L_1}{N\pi}\sqrt{\frac{2\omega\rho\eta}{\mu_q \rho_q}} \qquad (14)$$

and

$$L_2 = \frac{n\omega_s L_1}{N\pi}\sqrt{\frac{2\rho\eta}{\omega\mu_q\rho_q}} \quad (15)$$

Note that $R_2 \equiv \omega_s L_2$ for a Newtonian fluid. The liquid shear propagation constant, γ, can be related to the motional impedance elements as:

$$\gamma = \frac{4K^2\omega_s C_o\sqrt{\mu_q\rho_q}}{nN\pi\eta}(R_2 + j\omega_s L_2) \quad (16)$$

Thus, the equivalent circuit model for liquid-loaded resonators provides a relevant link to the energy storage and power dissipation in the radiated acoustic wave.

The total motional impedance for the mass and liquid loaded quartz resonator is

$$Z_m = (R_1 + R_2) + j\omega(L_1 + L_2 + L_3) + \frac{1}{j\omega C_1} \quad (17)$$

Combining this impedance with the capacitive reactances in the static branch leads to a description of the equivalent admittance (current/applied voltage) for the entire resonator system:

$$Y = j\omega(C_o + C_p) + \frac{1}{Z_m} \quad (18)$$

Typical values of the static capacitances are $C_o \approx 4.2$ pF and $C_p \approx 5$ to 10 pF, the latter depending on the mounting fixture.

The motional inductance contributed by a mass layer causes only a shift in resonant frequency. Using Eq. (12) in the equivalent circuit model gives

$$\Delta f_s \equiv -\frac{L_3 f_s}{2L_1} = -\frac{2f_s^2 n}{N\sqrt{\mu_q\rho_q}}\rho_s \quad (19)$$

which is equivalent to the Sauerbrey equation [5]. Mass sensitivities of less than 1 ng/cm^2 are possible with a 5 MHz resonator in a stable oscillator circuit (frequency fluctuations less than 1 Hz). The mass measurement capability of the resonator gives rise to the often used name "quartz crystal microbalance" or QCM.

Liquid loading produces both a frequency shift and a decrease in the admittance magnitude. Admittances for four fluid-loaded resonators near the fundamental resonance are shown in Fig. 4. Peak admittance magnitude for air in contact with the resonator is ~ 100 mmhos, or 30 times the displayed range. The three liquids represent those encountered in automotive systems and cover the spectrum of density-viscosity products: $\rho\eta$ = 0.01 to 0.882 at 20 ° C. As the value of $\rho\eta$ increases, the peak frequency is shifted by

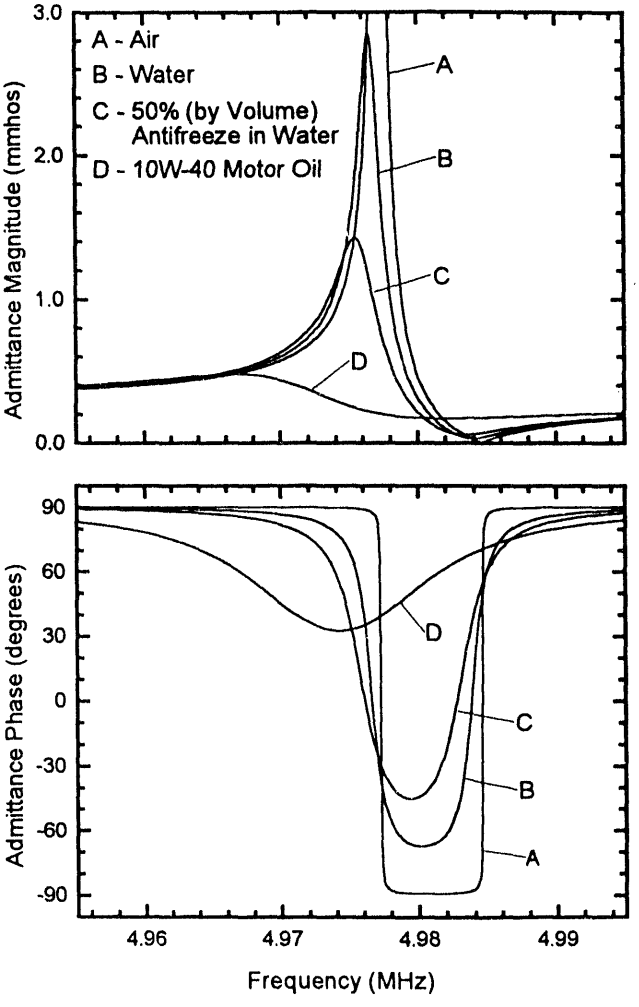

Fig. 4. Admittance magnitude and phase near the fundamental resonance showing the effects of increasing fluid density-viscosity: (A) air, $\rho\eta$ = 2 x 10-7; (B) water, $\rho\eta$ = 0.010; (C) 50% by volume antifreeze in water, $\rho\eta$ = 0.044; and (D) 10W-40 motor oil, $\rho\eta$ = 0.882. All $\rho\eta$ at 20 °C.

$$\Delta f_s = -\frac{f_s}{2}\left[1+\frac{N}{2n}\sqrt{\frac{\pi\mu_q\rho_q}{n f_s \rho\eta}}\right]^{-1} \quad (20)$$

while the peak admittance magnitude is reduced:

$$|Y_{max}| = \sqrt{4\pi^2 f_s^2 (C_o + C_p)^2 + \frac{1}{(R_1+R_2)}} \quad (21)$$

where

$$R_1 + R_2 = \frac{(N\pi)^2}{8K^2 C_o}\left[\frac{\eta_q}{\mu_q}+\frac{n}{N}\sqrt{\frac{\rho\eta}{\pi^3 f_s \mu_q \rho_q}}\right] \quad (22)$$

When liquid loading is not severe (R_2 is much less than the reactance produced by the static capacitances), then peak admittance magnitudes are approximated by $(R_1 + R_2)^{-1}$.

The density-viscosity can be determined by observing the response of the quartz resonator while contacting the fluid of interest. Contact can be only a few drops of a liquid on one side of the resonator or complete immersion. The acoustic wave decay length for water [Eq. (6)] is only 0.25 μm at 5 MHz; thus, a thin layer of a liquid is all that is required to make a measurement. An automatic network analyzer (ANA) can be used to scan the frequencies near resonance, a computational fit made to the equivalent-circuit-model admittance, Eq. (18), and the value of $\rho\eta$ extracted from either R_2 or L_2. Equivalently, the frequency shift and the damping of the peak admittance magnitude can be determined and $\rho\eta$ extracted using Eqs. (20) or (21). An alternate method for measuring $\rho\eta$ requires operating the quartz resonator as a control element in an oscillator circuit. Oscillator frequency approximates f_s when operated in air, and any damping of the oscillator signal near f_s relates to Y_{max} or the motional impedance, $\sim|Y_{max}|^{-1}$. Shifts in the measured parameters while in contact with the fluid can then be related to $\rho\eta$.

A single quartz resonator responds only to the density-viscosity product as described by Eqs. (14) and (15), and separating these two quantities is impossible. If each parameter must be known, an independent measurement of either ρ or η is required. This procedure, however, removes the advantages of *in situ* or real-time determination. It is possible to use two resonators, one with a smooth surface and other with a textured (randomly rough or regularly corrugated) surface to extract both density and viscosity separately [6, 7]. The smooth device acts as described previously to measure $\rho\eta$. The textured device traps an additional quantity of the liquid in the crevices so that it moves synchronously with the quartz surface and is "weighed." It becomes equivalent to a mass layer, which causes an additional frequency shift according to Eq. (19) where $\rho_s = \rho h_o$, h_o being the effective thickness of the trapped fluid. Density is determined from the difference in frequency responses between the textured and smooth devices. Knowing ρ, viscosity can be extracted from $\rho\eta$ of the smooth resonator response.

In this study of automotive fluid monitoring, little use of the dual resonators to measure density and viscosity separately has been attempted. All data presented in this paper is the result of $\rho\eta$ extraction from a single smooth device.

Oscillator Electronics

Quartz resonator liquid sensors require the use of specially-designed oscillator circuits. It is necessary for the oscillator to accommodate the high resistances due to liquid damping yet provide a predictable output over the wide dynamic range of resonator resistance. Standard oscillator designs, like the Pierce or Colpitts type, do not function well because of their inherent phase and gain sensitivity to the resonator loss. The "Lever oscillator" described here uses negative feedback in a differential amplifier configuration to actively and variably divide (lever) the resonator impedance as to maintain the oscillator phase and loop gain [8]. The oscillator servos the resonator impedance to a constant, nearly-zero phase over a wide dynamic range of resonator resistances (10 Ω to 5 kΩ). When using a 5 MHz resonator (fundamental mode), this dynamic range will allow single-sided measurements up to $(\rho\eta)^{1/2} \approx 1.6$ g/(cm^2-s$^{1/2}$).

A schematic of the Lever oscillator circuit is shown in Fig. 5. A single 5 volt supply is used to power the circuit; source drain is typically 20 mA. There are two signal outputs: a 200 mV_{p-p} RF signal with a frequency that corresponds approximately to

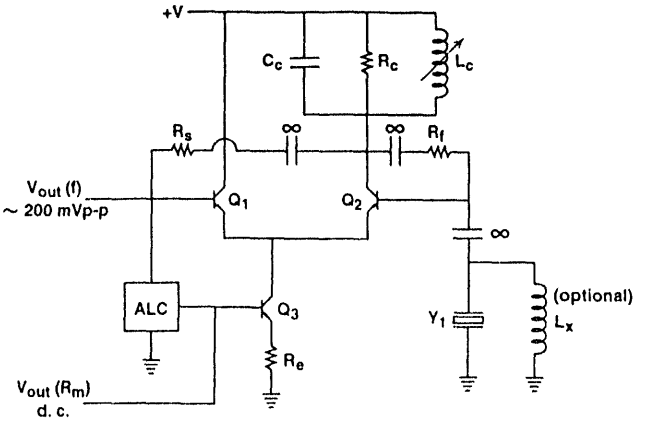

Fig. 5. The Lever oscillator circuit design with automatic level control (ALC).

the series resonance of the quartz-liquid system, f_s; and a d.c. voltage proportional to the system motional resistance, $R_1 + R_2$.

When operating at f_s, the resonator impedance is near minimum and is given by

$$Z_{res} = \left[j\omega_s (C_o + C_p) + \frac{1}{R_1 + R_2} \right]^{-1} \qquad (23)$$

If the motional resistance is small compared to the capacitive reactance, then the resonator impedance is essentially real and f_s is very close to the frequency at which the impedance phase is zero. The Lever oscillator attempts to maintain this condition so that open loop voltage gain, A_v, is independent of transistor β and is approximated by

$$A_v \approx \frac{R_c}{2h + \dfrac{R_c R_m}{R_c + R_f + R_m}} \geq 1 \qquad (24)$$

where R_c, R_m, and R_f are the collector resistance, resonator motional resistance ($R_1 + R_2$), and feedback resistance shown in Fig. 5, and h is the intrinsic emitter resistance of the amplifier transistors, Q_1 and Q_2 (at 25 °C, h = 26 mV / I_e, where I_e is the emitter current). The second term in the denominator of Eq. (24) is the "lever" term since it effectively divides the resonator impedance by the circuit elements R_c and R_f. Wide dynamic range, good sensitivity, and transistor independence is realized when $R_f/R_c << \beta$.

Resonator impedance phase is kept small by minimizing the effects of transistor capacitance in Q_2. The parallel L-C tank circuit across R_c makes the collector to ground impedance real at the desired operating frequency. This also prevents the circuit from jumping to a parasitic (capacitance controlled) frequency when resonator loss becomes large. The feedback impedance, Z_f, is also forced to be essentially real by selecting R_f to be much less than the collector-to-base capacitive reactance of transistor Q_2. Then, if $R_c << Z_f$, the resonator impedance phase follows approximately as the phase of Z_f. And with R_c and Z_f real, the resonator impedance must also be real to satisfy Eq. (24). Figure 6 shows the measured resonator impedance phase as a function of the magnitude of the resonator impedance for the Lever oscillator operating with a 6 MHz quartz resonator. Above 200 ohms the impedance phase is steady near 6°, which is approximately that determined by the phase of Z_f. The phase shift at low resonator impedances is caused by increased oscillator sensitivity to circuit parameters not included in the approximations used to determine component selection. Fortunately, for small resonator loss the resonator Q is extremely large and oscillator performance is not dependent on resonator impedance phase.

The automatic level control (ALC) circuit shown in Fig. 5 is designed to keep the oscillator gain constant by controlling the current source, Q_3. Indirectly, a measure of the control voltage indicates the resonator motional resistance. A plot of ALC output voltage versus resonator resistance is shown in

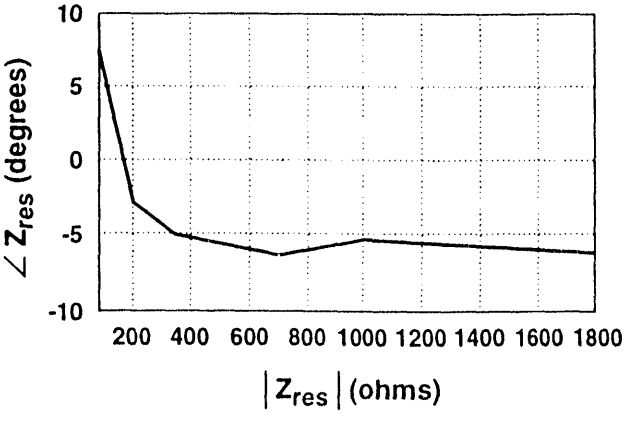

Fig. 6. Measured resonator impedance phase versus the magnitude of resonator impedance for a 6 MHz test device.

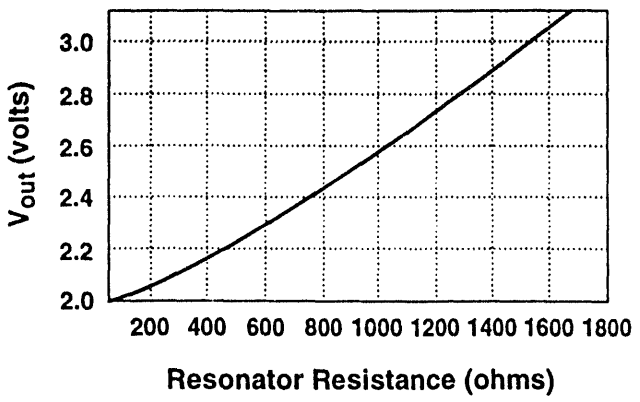

Fig. 7. Oscillator output voltage versus resonator resistance. Gain of the ALC can be adjusted for response to a large range of resonator resistances.

Fig. 7. The response is approximately linear with resonator damping up to 1700 ohms. Gain of the ALC can be adjusted to increase the range of resistance measurements. For highly viscous liquids such as lubricants, the resonator motional resistance can exceed 5000 ohms (see Fig. 10). The upper resistance limit for oscillator operation is increased dramatically by using the inductor, L_x, shown in Fig. 5, which effectively tunes out the static capacitance, $C_o + C_p$, of the resonator and its fixture.

Lubricating Oil Monitor

The ability of the quartz resonator monitor to indicate density-viscosity ($\rho\eta$) of fluids makes it a candidate for an *in situ*, real-time diagnostic for engine lubricating oil. Determination of lubricant viscosity is a standard analytical procedure [9] both in the formulation of products and in the characterization of lubricating quality during use. It is important to protect against excess wear in engines and machines, yet reduce costly maintenance and waste disposal. Several studies note changes in oil viscosity as a function of vehicle use [10-12]. Viscosity shifts result from oil thickening, emulsification, and fuel/water dilution.

Quartz resonator response in contact with lubricating oil is illustrated in Fig. 8. The admittance magnitude at three temperatures is plotted versus frequency for the resonator operating in 10W-40 motor oil. In Fig. 9, the extracted density-viscosity for temperatures between 0 to 100 °C is shown. As observed in both figures, lubricating oil exhibits a particularly strong dependence on temperature. Much of this variation is due to the large viscosity increases at the low temperatures. In Fig. 8 severe damping of the resonator signal occurs even at room temperature. From Fig. 9, $\rho\eta = 0.88$ g^2/cm^4-s at 20 °C. A separate density measurement on the 10W-40 oil at 20 °C gave 0.88 g/cm^3, indicating $\eta = 100$ cP. This value represents the approximate viscosity upper limit for Lever oscillator operation in conjunction with a resonator having single-sided liquid contact. Thus, high-precision characterization of oil properties is best performed at elevated temperatures where resonator Q and measurement signal-to-noise are large.

Standard laboratory analysis of lubricating oils extracts the kinematic viscosity, ν, instead of the dynamic viscosity, η. The relationship between the two quantities is $\nu = \eta/\rho$. Quartz resonator response is then related to the kinematic viscosity by $\rho\eta = \nu\rho^2$. At 20 °C, the kinematic viscosity of the previous 10W-40 oil sample is approximately 114 cSt (centistokes or mm^2/s). In order to characterize the temperature dependence of the viscosity (often referred to as viscosity index), a second density was measured for the 10W-40 oil at 64 °C. Interpolating the $\rho\eta$ data in Fig. 9, values for η and ν were then determined for this lubricating oil at this second temperature. Variation in the viscosity for petroleum products is described in the ASTM standard handbook [13, 14] and is given by the linearized

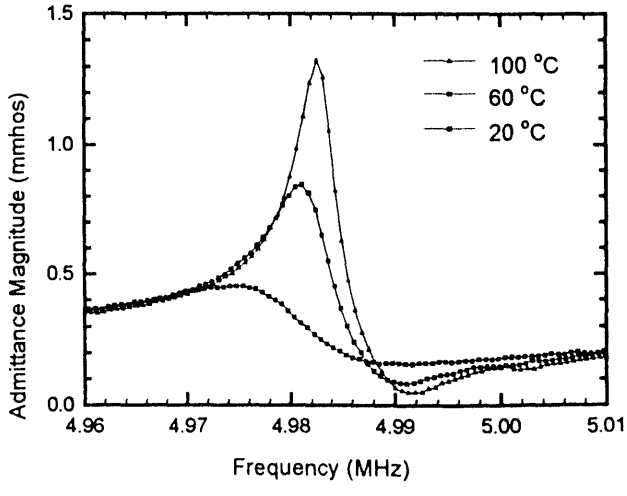

Fig. 8. Quartz resonator admittance magnitude for 10W-40 lubricating oil at three temperatures.

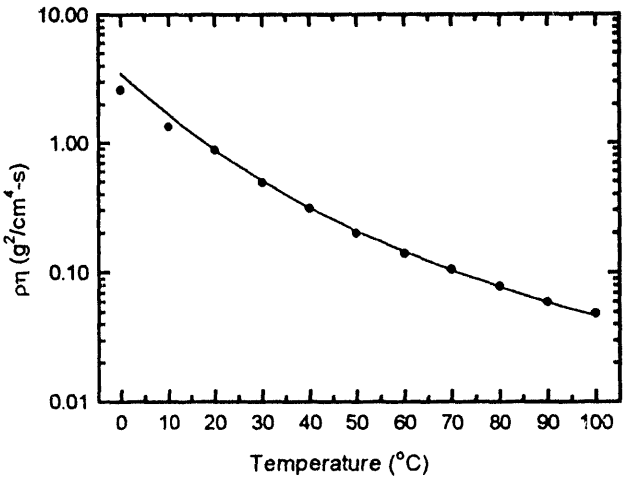

Fig. 9. The liquid density-viscosity product (●) extracted from resonator measurements in 10W-40 motor oil. The solid curve is a theoretical prediction for temperature variations based on ASTM Standard D341-93.

expression

$$\log\log(z) = A - B \bullet \log(T) \qquad (25)$$

where $z = \nu +$ (constant), T is the absolute temperature, and A and B are constants. The constant added to ν is 0.7 for $\nu \geq 1.5$ cSt, which is characteristic of lubricants up to ~ 200 °C [14]. Using the two values of kinematic viscosity at two different temperatures, A and B are determined from Eq. (25): A = 9.80, B = 3.48.

Temperature-dependent density variations in the 10W-40 oil are assumed due to simple dilatation, i.e., linear expansion in each direction:

$$\rho = \frac{\rho_o}{\left[1 + C(T - T_o)\right]^3} \qquad (26)$$

where ρ_o is the density at T_o, and C is the coefficient of linear expansion for the liquid. Values for the constants ρ_o, T_o, and C are determined from the two density measurements at 20 and 64 °C. Combining Eqs. (25) and (26) and substituting the appropriate fit parameters produces a theoretical expression for the temperature variations of $\rho\eta$ in the 10W-40 lubricating oil. This curve is plotted as a solid line in Fig. 9. Above 20 °C, the fit is excellent, having an average error of 1.6%. Below 20 °C, the measured values show increasing deviation from the curve-fit model as the temperature drops; the relative error is 35% at 0 °C. This discrepancy is almost entirely due to errors in the resonator determination of viscosity over this range; the viscosity at 0 °C is approximately 400 cP.

The response of a single quartz resonator appears adequate for characterizing lubricating oils where the density-viscosity product is a relevant indicator of fluid parameter variations. More precise characterization requires extraction of just the viscosity. As discussed previously, two resonators, one smooth and the other having a textured surface in contact with the liquid, can separate density and viscosity. Such a sensor system has yet to be tried with lubricants.

Many lubricating oils exhibit non-Newtonian characteristics, especially under high shear conditions or when operating at extreme temperatures. Initial developments of quartz resonator response assumed that liquids were strictly Newtonian. Then energy-storage and power-dissipative components of the motional impedance are simple functions of $\rho\eta$. Resonator theory can be extended to include shear rate dependence in the viscosity [15]:

$$\eta = \frac{\eta_o}{1 + j\omega\tau} \qquad (27)$$

where η_o is the low-frequency viscosity and τ is a shear relaxation time. For a Maxwell fluid, the relaxation time depends on the viscosity, with $\tau = \eta_o/\mu$, where μ is the high-frequency shear modulus for the liquid. For $\omega\tau << 1$, the liquid is purely Newtonian in behavior. But at high frequencies or for large viscosities, the non-Newtonian character is manifested in a separation of the real and imaginary parts of the liquid-induced motional impedance: $R_2 \neq \omega_s L_2$. This is in contrast to values extracted from Eqs. (14) and (15).

The non-Newtonian aspects of a liquid can be observed by plotting R_2 and $\omega_s L_2$ for increasing viscosity, or, equivalently, decreasing temperature. In Fig. 10, these two parameters are shown for two lubricants: a 10W-40 motor oil and a 50W racing oil. Both sets of curves show some separation in the impedance parameters. The 10W-40 oil is Newtonian above 40 °C, exhibiting some non-Newtonian behavior at and below room temperature. The 50W

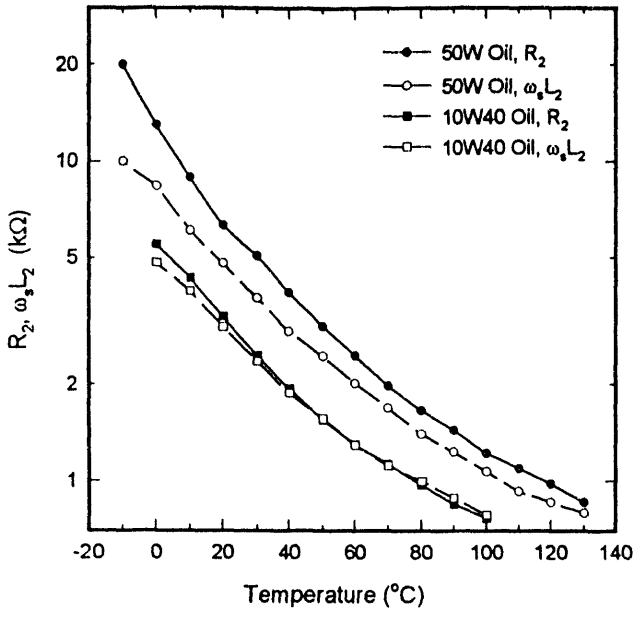

Fig. 10. The variation in motional impedance parameters versus temperature for two lubricating oils: 10W-40 and 50W.

oil shows Maxwell fluid characteristics over the entire measurement range. Only well above 140 °C is Newtonian response expected. Based on this limited data set, it appears that quartz resonator monitors have the ability to determine important non-Newtonian behavior in lubricants.

Battery State-of-Charge Monitor

The active materials in a lead-acid battery are lead oxide (PbO_2) on the positive plates, porous lead (Pb) on the negative plates and dilute sulfuric acid (H_2SO_4) as the electrolyte [16]. During the discharging and charging of the battery, the chemical reaction in each cell is described by

$$PbO_2 \text{ (Anode)} + 2\,H_2SO_4 \text{ (Electrolyte)} + Pb \text{ (Cathode)}$$
$$\text{discharge} \downarrow \uparrow \text{charge}$$
$$PbSO_4 \text{ (Anode)} + 2\,H_2O \text{ (Electrolyte)} + PbSO_4 \text{ (Cathode)}.$$

The concentration of sulfuric acid in the electrolyte changes significantly with the battery state-of-charge. Approximate concentration ranges for fully charged and discharged states are shown along the abscissa in Fig. 11 [16, 17].

Both the density and viscosity of the battery electrolyte vary with the H_2SO_4 concentration. Literature values of these two parameters are plotted (solid lines) in Fig. 11 [18]. Traditionally, electrolyte density has been used to indicate state-of-charge in a lead-acid battery, although viscosity exhibits a much stronger dependence on acid concentration (5.5 times the sensitivity at 40% H_2SO_4). The quartz resonator response, proportional to $(\rho\eta)^{1/2}$, is also plotted. Figure 11 shows that density-viscosity values measured with the quartz monitor (open circles) agree with literature values (solid line). Because of the conductivity of the sulfuric acid, only one surface of the quartz resonator can be exposed to the liquid to avoid "shorting" between electrodes.

In a laboratory demonstration, a small 12V lead-acid battery was discharged and recharged several times in succession. The electrolyte in one cell was continuously pumped across the surface of the quartz resonator. The Lever oscillator circuit was used in conjunction with the resonator and provided the electrical signals for monitoring the frequency shift and the damping magnitude. Periodically, the electrolyte specific gravity was measured using a float hydrometer. Since density and viscosity are temperature dependent, a separate measurement of temperature was also made.

Four parameters extracted from one discharge cycle in the test series are plotted in Fig. 12. The quartz oscillator voltage tracks quite precisely both

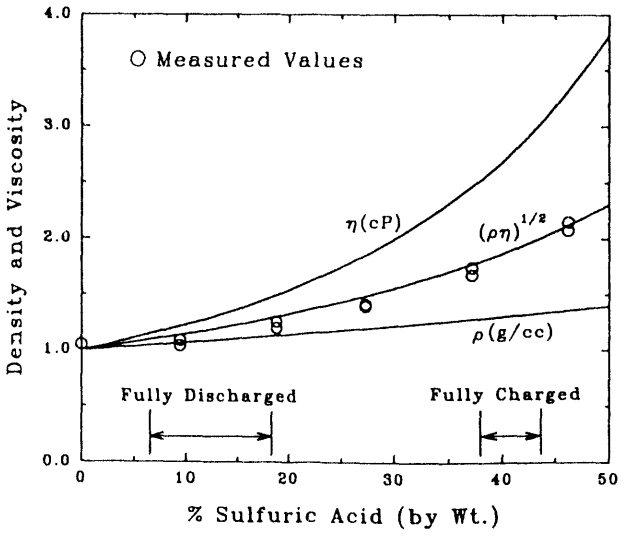

Fig. 11. Parameter variations for the electrolyte in a lead-acid cell as a function of the sulfuric acid concentration.

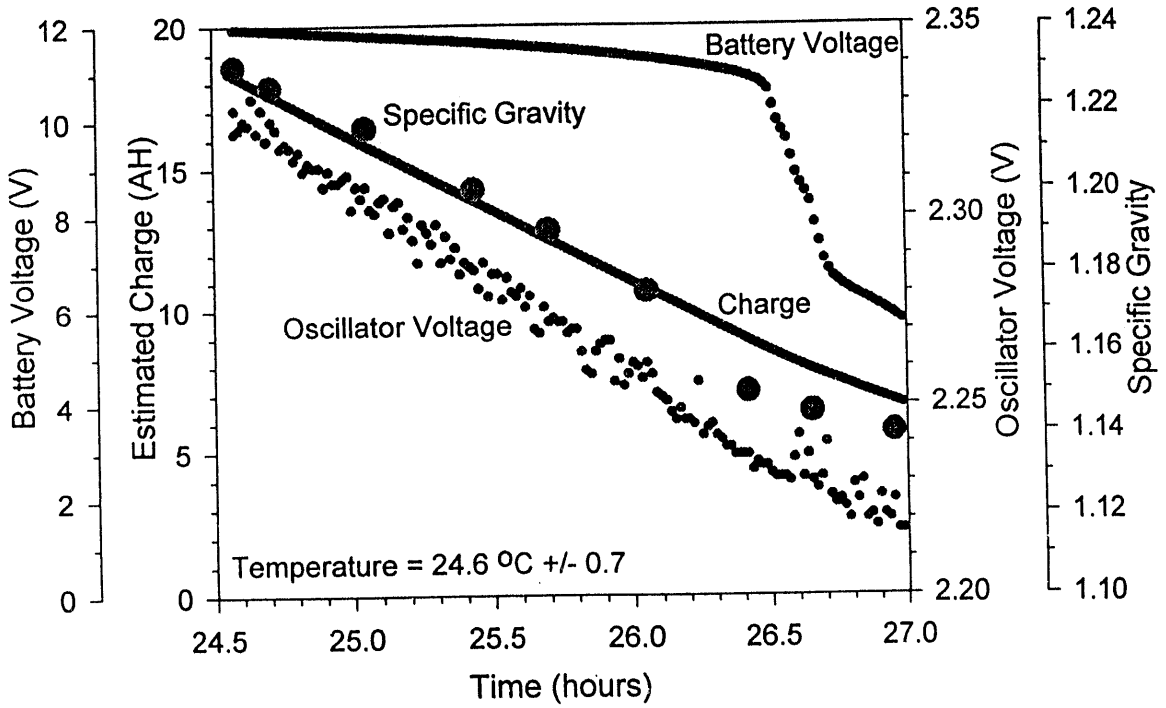

Fig. 12. Changes in the battery parameters and the sensor voltage output versus time for one deep discharge cycle in a test series.

the electrolyte specific gravity and the estimated charge (battery discharge current × time). Estimating the charge alone could be used to indicate state-of-charge, except this parameter can be highly charge/discharge-rate dependent and initial charge conditions must be known *a priori*. The battery voltage is also plotted in Fig. 12. Battery voltage is not a good measure of the state-of-charge, showing little deviation for most of the discharge cycle and then falling catastrophically as the charge depletes. The correlation among the estimated charge capacity of the battery, the electrolyte density and the measured quartz monitor voltage is quite high. Coefficients for pairings of these parameters are given in Table 1. These high correlation coefficients are an indication this monitor has the potential for accurately measuring state-of-charge.

Table 1. Correlation coefficients among three of the battery and sensor parameters plotted in Fig. 12

Correlating Parameters	Coefficient
Specific Gravity ↔ Estimated Charge	0.982
Oscillator Voltage ↔ Estimated Charge	0.984
Specific Gravity ↔ Oscillator Voltage	0.993

The shift in resonant frequency of the monitor proved to be an unreliable measurement for determining electrolyte density-viscosity and, consequently, battery state-of-charge. Small quantities of lead oxides and salts from the electrolyte intermittently settled onto the resonator surface. This produced a frequency shift due to the accumulated surface mass. Oscillator voltage, which depends only on the viscous damping contributed by the liquid, does not respond to these changes in surface mass. Thus, a simple oscillator damping measurement is all that is required for this monitor.

The laboratory tests demonstrated that a TSM quartz resonator can be used as a real-time, *in situ* monitor of the state-of-charge of lead-acid batteries. Quartz resonators are small in size, compatible with the corrosive electrolyte environment, and can be easily configured to fit into each of the cells. This type of monitor is more precise than sampling

hydrometers since it responds to changes in both the density and viscosity of the sulfuric acid electrolyte. It is proposed that quartz resonator monitors can provide real-time metering of state-of-charge in present vehicle storage batteries and serve as the sensor for a "fuel gauge" in electric vehicle power sources.

Coolant Capacity Monitor

Typical vehicle cooling systems contain solutions of a primary agent (mostly ethylene glycol) and water. The capacity of this coolant to perform properly yet resist freezing under non-operating conditions depends on the component concentrations in solution. Figure 13 shows several properties of ethylene glycol at varying concentrations in water [18]. Recommended antifreeze/coolant mixtures for most vehicles is 50% by volume (52% by weight) in water, giving freezing-point protection to -40 °C.

Present coolant monitoring systems check capacity or freezing-point protection by measuring the solution density. Like in the battery system discussions in the previous section, density monitoring requires drawing a sample using a hydrometer (floating ball or float level). Density measurements can be performed quite accurately and provide a good indicator of capacity. As observed in Fig. 13, however, the viscosity of ethylene glycol solutions is a much stronger function of concentration than is the density, being approximately 100 times more sensitive to changes near 50% concentration. Since the quartz resonator monitor responds directly to $(\rho\eta)^{1/2}$, it can take advantage of this increased sensitivity. Ability to operate *in situ* and to provide information in real-time are added advantages.

Figure 14 displays plots of the measured and literature values for ρ and $(\rho\eta)^{1/2}$. The quartz resonator response (open circles), determined for a commercial antifreeze/coolant, are in good agreement with the literature values for pure ethylene glycol. Some discrepancies in the curves are expected since commercial antifreeze contains small amounts of chemicals other than ethylene glycol. In fact, the measured densities for the antifreeze mixtures (closed circles in Fig. 14) were consistently 1 to 2% higher than literature values for pure ethylene glycol in water. It is obvious that coolant monitors must account for a range of responses since proprietary additives in commercial products can affect liquid properties.

A 5 MHz quartz resonator was used with the Lever oscillator to monitor characteristics of typical antifreeze mixtures. Concentration was varied from 0 to 50% by volume in water; temperature was varied between 0 and 100 °C, the exact range depending on

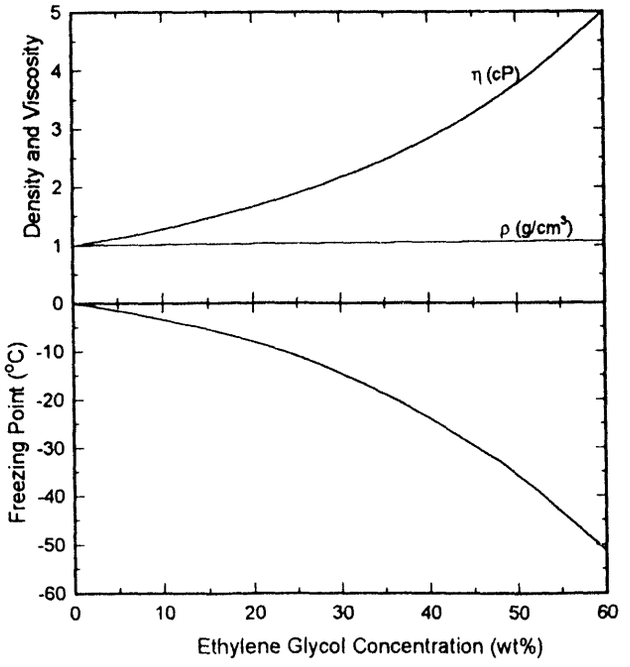

Fig. 13. Parameter variations for aqueous solutions of ethylene glycol as a function of concentration. Literature values are density, viscosity and freezing point at 20 °C.

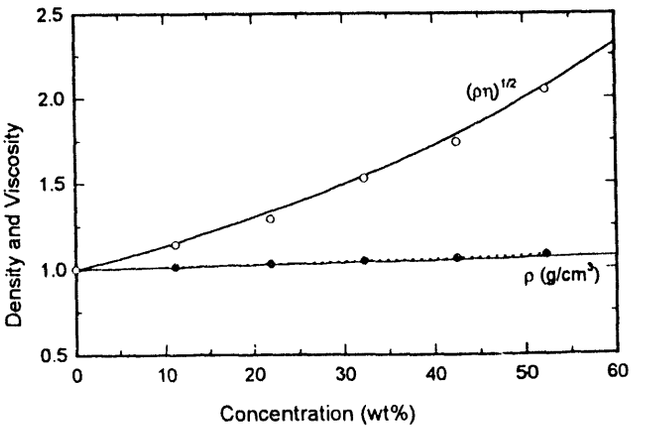

Fig. 14. Quartz resonator measurements (O) of $(\rho\eta)^{1/2}$ for commercial antifreeze solutions at 20 °C. Measured densities (●) are determined separately. Solid lines are literature values from Ref. 18.

the solution concentration. In Fig. 15, the oscillator frequency and voltage shifts are plotted versus concentration for three distinct temperatures for each mixture. Maximum shifts occur in both parameters at 10 °C (open circles) since densities and viscosities are greatest at that temperature. For the 50% solution at 10 °C, the liquid viscosity is large enough (estimated to be 7.5 cP) that oscillation at the fundamental frequency of the quartz resonator could not be maintained. A reconfiguration of the oscillator circuit components is required for continued operation at this higher viscosity (or higher motional resistance) range.

It is possible to measure either the voltage shift or the frequency shift from the monitor in vehicle antifreeze/coolant to provide an indication of the system capacity. As in the battery electrolyte monitor system, voltage response is expected to be more accurate since it is directly proportional to $(\rho\eta)^{1/2}$, while frequency response has an added contribution due to mass deposition. Rust and corrosion particulates that are likely to form in vehicle cooling systems could settle on the resonator surface and skew density-viscosity measurements made with frequency shift only.

The quartz resonator monitor also has the ability

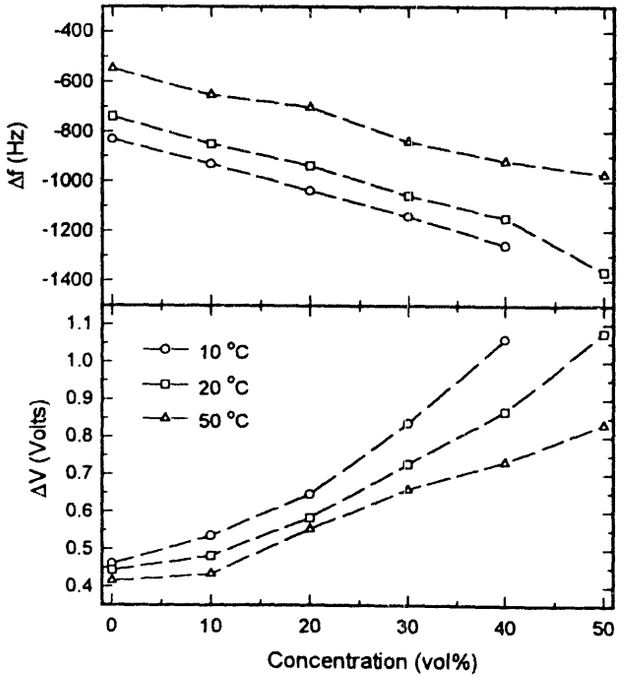

Fig. 15. Oscillator circuit frequency and voltage shifts measured at three temperatures (10, 20 and 50 °C) for varying volume concentrations of antifreeze in water.

to determine phase changes in materials contacting the surface. Changes in the properties of a liquid as it transforms to the solid phase are captured by dramatic shifts in both resonator operating frequency and resonance damping. An icing monitor is constructed by spreading a thin layer of water (or modified water solution) over the quartz surface. Immediate response to solidification is evident. By strategically placing a quartz monitor in a vehicle cooling system, it would be capable of predicting fluid freezing prior to bulk ice formation that could seriously damage an engine.

Conclusion

We have investigated the capability of TSM quartz resonators as a diagnostic monitor for three fluids used in vehicle systems: engine lubricating oil, battery electrolyte, and engine coolant. In each case, the sensor responds to changes in the liquid density-viscosity product due to temperature variation, concentration shifts, or a combination of these. Mass deposition on the quartz surface and phase changes in the contacting liquid also produce shifts in the sensor response, although these parameters have not yet been quantified as part of this study. The quartz resonator monitor can track viscosity changes in lubricants and potentially can separate non-Newtonian from Newtonian fluid characteristics. Real-time monitoring of lead-acid battery state-of-charge was demonstrated during charge/discharge cycling of an actual battery. Predictable resonator responses to concentration and temperature changes in antifreeze solutions verified its capability as an *in situ* coolant monitor.

The quartz resonator technology can be extended to monitor other vehicle fluids — transmission and brake fluids, for example — as well as to explore new properties and characteristics of the three fluids presently under investigation. The technology can also be utilized in other operating modes (i.e., thin-film coated resonators) to explore liquid or gas chemistry. A wide range of applications in the automotive industry appear possible.

References

[1] C. E. Reed, K. K. Kanazawa and J. H. Kaufman, "Physical Description of a Viscoelastically Loaded AT-Cut Quartz Resonator," *J. Appl. Phys*, **68**, pp. 1993-2001 (1990).

[2] F. M. White, "Fluid Oscillation above an Infinite Plate," Sec. 3-5.1 in *Viscous Fluid Flow* (McGraw-Hill, New York, 1991).

[3] K. K. Kanazawa and J. G. Gordon, "Frequency of a Quartz Microbalance in Contact with Liquid," *Anal. Chem.*. **60**, pp. 1770-1771 (1988).

[4] S. J. Martin, V. E. Granstaff and G. C. Frye, "Characterization of a Quartz Crystal Microbalance with Simultaneous Mass and Liquid Loading," *Anal. Chem.*, **63**, pp. 2272-2281 (1991).

[5] G. Sauerbrey, "Verwendung von Schwingquarzen zur Wägung dünner Schichten and zur Mikrowägung (Application of Vibrating Quartz to the Weighing of Thin Films and Use as a Microbalance)," *Z. Phys.*, **155**, pp. 206-222 (1959).

[6] S. J. Martin, G. C. Frye, A. J. Ricco and S. D. Senturia, "Effect of Surface Roughness on the Response of Thickness-Shear Mode Resonators in Liquids," *Anal. Chem.*, **65**, pp. 2910-2922 (1993).

[7] S. J. Martin, G. C. Frye, R. W. Cernosek and S. D. Senturia, "Microtextured Resonators for Measuring Liquid Properties," *Proc. Sensors and Actuators Workshop*, Hilton Head Is., S.C. (1994).

[8] K. O. Wessendorf, "The Lever Oscillator for Use in High Resistance Resonator Applications," *Proc. 1993 IEEE Intl. Freq. Control Symp.*, pp. 711-717 (1993).

[9] American Society for Testing and Materials (ASTM), "Kinematic Viscosity of Transparent and Opaque Liquids (and the Calculation of Dynamic Viscosity)," D445-83, *Annual Book of ASTM Standards* (Philadelphia, 1994).

[10] N. E. Gallopoulos, "Engine Oil Thickening in High-Speed Passenger Car Service," *SAE Transactions*, **79**, SAE paper #700506 (1970).

[11] S. E. Schwartz, "Observations Through a Transparent Oil Pan During Cold-Start, Short-Trip Service," *Int'l Fuels and Lubricants Meeting and Exposition*, Toronto, SAE paper # 912387 (1991).

[12] S. E. Schwartz, "A Comparison of Engine Oil Viscosity, Emulsion Formation and Chemical Changes for M85 and Gasoline-Fueled Vehicles in Short Trip Service," *Int'l Fuels and Lubricants Meeting and Exposition*, San Francisco, SAE paper # 922297 (1992).

[13] American Society for Testing and Materials (ASTM), "Standard Viscosity-Temperature Charts for Liquid Petroleum Products," D341-93, *Annual Book of ASTM Standards* (Philadelphia, 1994).

[14] W. A. Wright, "An Improved Viscosity-Temperature Chart for Hydrocarbons," *J. of Materials*, **JMLSA 4**, No. 1, pp. 19-27 (1969).

[15] J. R. Van Wazer, J. W. Lyons, K. Y. Kim and R. E. Colwell, "Viscoelastic Theory, Mechanical Models Without Mass," in *Viscosity and Flow Measurement* (J. Wiley & Sons, New York, 1963).

[16] V. S. Bagotzky and A. M. Skundin, "Lead (Acid) Storage Cells," Ch. 10 in *Chemical Power Sources* (Academic Press, New York, 1980).

[17] F. Meyer, "Electrical Energy Supply in the Motor Vehicle," in *Automotive Handbook*, 3rd Edition, U. Adler, Chief Ed., (Bosch, Stuttgart, Germany, 1993).

[18] A. V. Wolf, M. G. Brown and P. G. Prentiss, "Concentrative Properties of Aqueous Solutions: Conversion Tables," *Handbook of Chemistry and Physics, 54th Edition*, R. C. Weast, Ed., pp. D-194 to D-236 (CRC Press, Cleveland, 1973).

DISCLAIMER

DATE
FILMED
10/28/94

END